# "Effect of elemental sulfur and sulfide on corrosion behavior of Cr-Mo low alloy steel for tubing and tubular components in oil and gas industry"

Ladan Khaksar[1], John Shirokoff[2]

[1] Department of Mechanical Engineering, Faculty of engineering and Applied Science, Memorial University of Newfoundland, St. John', NL, Canada, A1B3X5.

[2] Department of Process Engineering, Faculty of engineering and Applied Science, Memorial University of Newfoundland, St. John', NL, Canada, A1B3X5.

lk6514@mun.ca, shirokof@mun.ca

**Abstract.** The chemical degradation of stainless steel components in sulfur-containing environments is a major concern in oil and gas production. 4130 Cr-Mo alloy steel is widely used as tubing and tubular components in sour services. According to the previous research in aqueous conditions, contact of solid sulfur with alloy steel can initiate catastrophic corrosion problems. This paper discusses the effect of elemental sulfur and its simplest anion, sulfide, on corrosion of Cr-Mo alloy steel at pH 2 and 5 during 10, 20 and 30 hours immersion in two different solutions. The corrosion behavior was monitored by potentiodynamic polarization technique during the experiments. Energy dispersive x-ray spectroscopy (EDS), and scanning electron microscopy (SEM) have been applied to characterize the corrosion products after each experiment. The results show that under the same experimental conditions, the corrosion resistance of Cr-Mo alloy in presence of elemental sulfur is significantly lower than its resistance in presence of sulfide ions.

## 1. Introduction

For more than 40 years elemental sulfur deposition in pipeline and facilities has become a major concern in the sour oil and gas industry[1]. In conjunction with reservoir souring, the incidence of sulfur corrosion will likely increase. It is known from prior research that the presence of dry elemental sulfur in contact with carbon steel is not considered as a corrosion threat to steel, however by adding water to the system, the corrosion process may be dramatically accelerated [2].

Elemental sulfur usually appears in aqueous system due to oxidation of sulfide species where the possible reaction for the formation of elemental sulfur ($S_8$) may involve high oxidation state metals or oxygen[3]:

$$8\,H_2S\,(aq) + 16\,Mn^{+}\,(aq) \rightarrow S_8\,(s) + 16\,H^{+}\,(aq) + 16\,M^{(n-1)+}\,(aq) \tag{1}$$

$$8\,H_2S\,(aq) + 4\,O_2\,(g) \rightarrow S_8\,(s) + 8\,H_2O\,(l) \tag{2}$$

It was identified by Boden et al. that acidification in sulfur containing aqueous systems is one of the main factors governing corrosion in the presence of elemental sulfur[4]:

$$S_8\,(s) + 8H_2O\,(l) \rightarrow 6\,H_2S\,(aq) + 2\,H_2SO_4\,(aq) \tag{3}$$

Besides of this acidification theory, MacDonald et al. hypothesized that an electrochemical reaction between iron and polysulfide is the driving force for corrosion process where elemental sulfur is present [5]:

$$(x\text{-}1)Fe + S_{v\text{-}1}\,.S^{2-} + 2\,H^{+} \rightarrow (x\text{-}1)\,FeS + H_2S + S_{v\text{-}x} \tag{4}$$

In recent years, Fang et al. investigated the corrosion behavior of carbon steel at different temperature by molten covering sulfur on steel surface [1], [6]. These investigations comprehensively studied the sulfur hydrolysis and direct sulfur/iron reaction, with either an electrically insulating or conductive barrier placed between the sulfur droplet and the metal surface.

Fang et al. investigation proved that the electrical connection and physical proximity between sulfur and steel are critical characteristics for elemental sulfur corrosion of mild steel. They also identified that an electrochemical reaction is the likely mechanism of elemental sulfur corrosion of mild steel. However, there are few electrochemical investigations on corrosion behavior of alloy under various environmental conditions IN presence of elemental sulfur in the simulated sour environment. In this paper, the effect of elemental sulfur and its anion on corrosion mechanism and behavior of the Cr-Mo low alloy steel were investigated at varying pH levels and immersion time through corrosion simulation test and electrochemical measurements.

## 2. Experimental procedure

### 2.1 Material and sample preparation

According to NACE MR0175/ISO 15156, the most common steel alloys for tubular and tubular components in sour service is UNS G41XX0, formerly AISI 41XX [7]. 4130 Steel is among the most common low alloys used in oil and gas industry. This steel typically consist of 0.80-1.1 Cr, 0.15-0.25 Mo, 0.28-0.33 C, 0.40-0.60 Mn, 0.035 P, 0.040 S, 0.15-0.35 Si and balance Fe. The working electrode was machined from the parent material into cylinders having dimensions of approximately 9 mm length and 9 mm diameter. Prior to the experiments, all specimens were polished with Coated Abrasive Manufacturers Institute (CAMI) grit designations 320, 600, 1000 corresponding to average particle diameters 36.0, 16.0, and 10.3 microns and finally 6-micron grit silicon carbide paper, and then cleansed with deionized water until a homogeneous surface was observed. Following this, the specimens were quickly dried using cold air to avoid oxidation.

### 2.2 Direct sulfur/ iron and sulfide/ iron reactions preparation

Two series of experiments have been performed to investigate the effect of elemental sulfur ($S_8$) and its simplest anion, sulfide ($S^{2-}$), on corrosion mechanism of Cr-Mo low alloy steel at varying pH and immersion time. At the first series of experiments, all of the tests were carried out in a multi-port glass cell which was filled with solved thioacetamide (2M) in 420 ml de-ionized water. Following equation shows the presence of dissolved free sulfides in the solution which are super active to react with samples. Table 1 describes the experimental conditions of first series of experiments.

$$CH_3SCNH_2 + H_2O \leftrightarrow S^{2-} + CH_3SCONH_2 + 2H^+ \tag{5}$$

Table 1. Experimental condition of first series.

| Condition No. | T (°C) | pH | Time (h) |
|---|---|---|---|
| 1 | 80 | 2 | 10 |
| 2 | 80 | 2 | 20 |
| 3 | 80 | 2 | 30 |
| 4 | 80 | 5 | 10 |
| 5 | 80 | 5 | 20 |
| 6 | 80 | 5 | 30 |

In the second series, a similar method to Fang et al. with maximum uniform coverage of adherent sulfur to the coupon surface was employed for all of the tests [1,4,6,8]. In this entire series of experiments, sublimed elemental sulfur 99.9999% (ACROS) was deposited onto polished samples. After preparing the samples, they were transferred into a multi-port glass cell which was filled with the 3.5% sodium chloride solution. Table 2 describes the experimental conditions of the second series of experiments.

Table 2. Experimental condition of second series.

| Condition No. | T (°C) | pH | Time (h) |
|---|---|---|---|
| 7 | 80 | 2 | 10 |
| 8 | 80 | 2 | 20 |
| 9 | 80 | 2 | 30 |
| 10 | 80 | 5 | 10 |
| 11 | 80 | 5 | 20 |
| 12 | 80 | 5 | 30 |

## 2.3 Electrochemical reactions

There are a number of electrochemical reactions that take place in first and second series of experiments. The reduction of $H^+$ is considered one of the key cathodic processes which is usually limited by how fast the $H^+$ can be transported from the bulk solution to the steel surface through the mass transfer boundary layer and the FeS(s) layer where present.

The direct reduction of water is another possible pathway for hydrogen evolution. This reaction is very slow compared

$$2H^+ + 2e \rightarrow H_2 \tag{6}$$

to the above cathodic reaction and commonly is neglected in estimating effects of practical sulfur-containing corrosion

$$2H_2O + 2e \rightarrow H_2 + 2OH^- \tag{7}$$

environments.

For the anodic reaction, there is often only one dominant anodic reaction (at the corrosion potential) involved in the corrosion process. Iron oxidation is the anodic reaction of low alloy steel in sulfur-containing environments [9].

## 2.4 Electrochemical measurements

$$Fe \rightarrow Fe^{2+} + 2e \tag{8}$$

Electrochemical corrosion experiments, and in particular, the potentiodynamic polarization scan, provide considerable information on the corrosion rate, pitting susceptibility, passivity as well as the cathodic behavior of an electrochemical system to be obtained [10]. During this study, experiments were conducted in a multi-port glass cell with a three electrode setup at atmospheric pressure based on the ASTM G5-82 standard for potentiodynamic anodic polarization measurements [11].

A graphite rod was used as the counter electrode (CE) and saturated silver/ silver chloride (Ag/AgCl) was used as the reference electrode (RE). In order to investigate the electrochemical characteristic of the corrosion films formed 4130 Cr-Mo alloy steel samples were used as working electrodes (WE).

An Ivium Compactstat Potentiostat monitoring system was used to perform electrochemical corrosion measurements. Potentiodynamic polarization technique was applied to investigate the corrosion mechanisms. The applied scan rate for this measurements was 0.125 mV/s. All the corrosion tests were conducted by setting the potentiostat to take measurements 10, 20 and 30 hours after the start of the tests. Prior to the start of each test, the sample was immersed in the solution for 55 minutes in accordance with ASTM G5-82 [11]. The pH was adjusted by adding deoxygenated hydrochloric acid or sodium hydroxide.

## 2.5 Surface morphology observation and corrosion product analysis

Upon completion of corrosion testing, morphological characterization of the surface was conducted using a FEI Quanta 400 scanning electronic microscope (SEM) with Bruker energy dispersive x-ray (EDS) spectroscopy. The SEM was operating at 15 kV, with a working distance of 15 mm, and beam current of 13 nA.

## 3. Results and discussion

### 3.1 First series of experiments; Effect of sulfide ($S^{2-}$) on corrosion mechanism of Cr-Mo low alloy steel

As it was mentioned in the experimental procedure in order to investigate the effect of sulfide ($S^{2-}$) on corrosion behavior of 4130 alloy, the samples were immersed into the solution containing solved thioacetamide (2M) in 420 ml de-ionized water.

### 3. 1. 1 Corrosion behavior of Cr-Mo low alloy steel

The potentiodynamic curves of 4130 Cr-Mo low alloy steel in thioacetamide solution at different immersion time: 10, 20 and 30 hours are illustrated in Figure 1. The scan rate was 0.125 mV/s.

Figure 1.indicates the stable behavior of anodic curves with increasing the immersion time from 10 to 30 hours at 80 °C, pH 2. It illustrated that Ecorr at pH 2 for 20 and 30 hours immersion time are almost the same and more positive than that of 10 hours immersion in the solution, however, the difference is not too much. It can be observed that current density of 10 hours immersion is higher than those of 20 and 30 hours immersion.
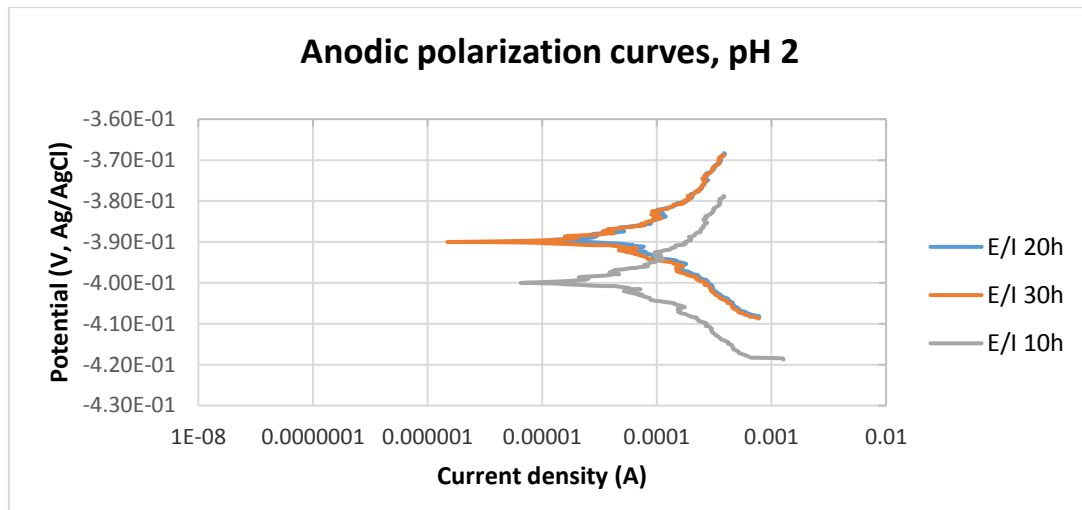
Figure 1. The potentiodynamic curves of 4130 Cr-Mo alloy steel in thioacetamide solution at different immersion time: 10, 20 and 30 hours at pH 2.

Figure 2.shows the stable behavior of anodic curves with increasing the immersion time from 10 to 30 hours at 80 °C, pH 5. The potentiodynamic polarization curves indicate that $E_{corr}$ of 10 hours immersion was relatively more positive than that of 30 hours immersion which was more positive than that of 20 hours. The current density of 10 hours immersion is slightly lower than that of 30 hours immersion time which is significantly higher than the current density of 20 hours immersion in the solution.
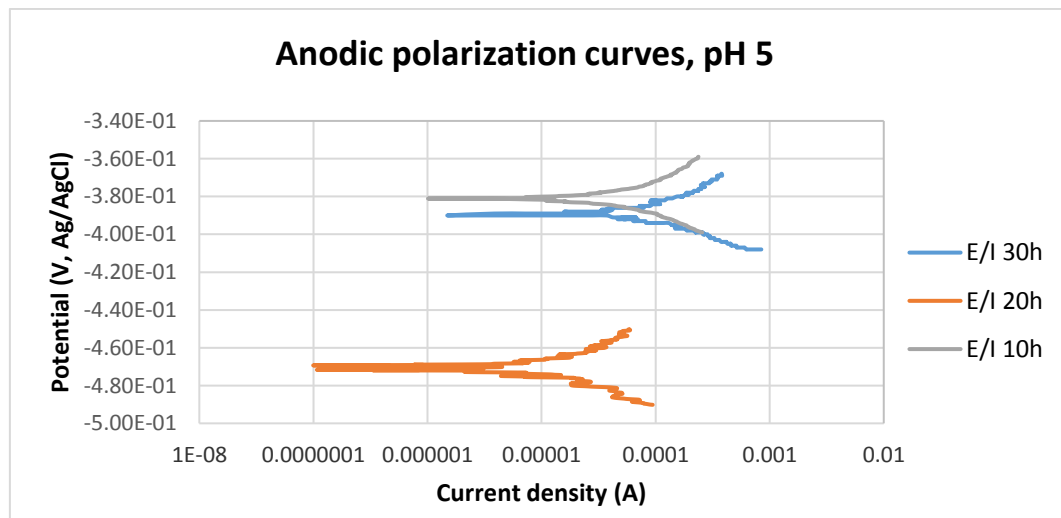


Figure 2. The potentiodynamic curves of 4130 Cr-Mo alloy steel in thioacetamide solution at different immersion time: 10, 20 and 30 hours at pH 5.

During a corrosion process, the rate of the reactions is determined by the corrosion mechanism. The growth of a corrosion film limits the rate of further corrosion by acting as a diffusion barrier for the species involved in the process [11- 12]. It can be said that after 20 hours immersion at pH 5, the formation of a protective corrosion layer prevented its subsurface from further corrosion however after 30 hours immersion, the corrosion current density significantly increased which may be related to breaking down of protective corrosion layer on the alloy surface. The values of anodic ($\beta_a$) and cathodic ($\beta_c$) Tafel slopes of the samples of each experiments were obtained by potentiostat as illustrated in Table 3.

Table 3. The values of anodic ($\beta_a$) and cathodic ($\beta_c$) Tafel slopes of first series.

| Experiment | $\beta_a$ (mV.decade $^{-1}$) | $\beta_c$ (mV.decade $^{-1}$) |
|---|---|---|
| 1 | 0.022 | 0.019 |
| 2 | 0.029 | 0.020 |
| 3 | 0.020 | 0.019 |
| 4 | 0.034 | 0.023 |
| 5 | 0.021 | 0.018 |
| 6 | 0.028 | 0.020 |

### 3.1.2 Corrosion rate of Cr-Mo low alloy steel

The corrosion current ($i_{corr}$) was calculated by using following equations[14]:

$$i_{corr} = \frac{B}{R_P}$$
(9)

Where:

$i_{corr}$ is the corrosion current density in A.$m^{-2}$;

$R_P$ is the polarization resistance in $\Omega.m^2$ and B is the proportionality constant in mV.decade–1:

$$B = \frac{\beta_a\,\beta_c}{2.3\,(\beta_a + \beta_c)}$$

Which can be calculated by given values of anodic ($\beta_a$) and cathodic ($\beta_c$) Tafel slopes of the samples of each experiments.

Finally the corrosion rate (CR) was calculated by using following equation:

$$CR = \frac{i_{corr}\,w}{\rho\,F}$$
(11)

Where:

w is the equivalent weight of 4130 alloy,

F is Faraday constant, and $\rho$ is the density of 4130 alloy.

Table 4 indicates the corrosion rate of each experiments.

Table 4. The corrosion rate of first series.

| Experiment | 1 | 2 | 6 | 4 | 5 | 6 |
|---|---|---|---|---|---|---|
| pH | 2 | 2 | 2 | 5 | 5 | 5 |
| Corrosion Rate-CR (mm/year) | 0.368 | 0.325 | 0.318 | 0.066 | 0.044 | 0.224 |

As it can be observed in Table 4 that in thioacetamide solution the corrosion rates of Cr-Mo alloy at pH 2 are greater than that of pH 5 which is usually related to the formation of corrosion protective layer at higher pH. At pH 2, iron is dissolved and iron sulfide is not precipitated on the surface of the alloy too much due to the high solubility of iron sulfide phases at pH values less than 2 [15]. In this case, sulfide exhibits only the accelerating effect on the dissolution of iron. At pH 5, inhibitive effect of sulfide is seen due to the formation of the iron sulfide protective film on the alloy surface [15].

The corrosion rate after 10 hours immersion at pH 2 has its maximum of 0.368 mm/y which slightly decreased to 0.318 mm/y after 30 hours immersion. The corrosion rates of pH 5 indicate a small decrease and a large increase during 20 and 30 hours immersion respectively due to formation and breakdown of corrosion product layer. These results are consistent with data obtained from potentiodynamic polarization technique.

### 3.2 Second series of experiments; Effect of elemental sulfur ($S_8$) on corrosion mechanism of Cr-Mo low alloy steel

As it was mentioned in the experimental procedure in order to investigate the effect of elemental sulfur ($S_8$) on corrosion behavior of 4130 Cr-Mo alloy, the surface of the samples were covered by melted elemental sulfur 99.999% (ACROS) and then immersed into a glass cell which was filled with the 3.5% sodium chloride solution.

### 3. 2. 1 Corrosion behavior of Cr-Mo low alloy steel

The potentiodynamic curves of 4130 Cr-Mo low alloy steel covered with elemental sulfur in the 3.5% sodium chloride solution at different immersion time: 10, 20 and 30 hours are illustrated in Figure 3. The scan rate was 0.125 mV/s. Figure 3.presents that $E_{corr}$ at pH 2 for 20 hours immersion time is more positive than that of 30 hours immersion in the solution, however, the difference is not too much. It can be observed that current density of 30 hours immersion is higher than that of 20 hours immersion.
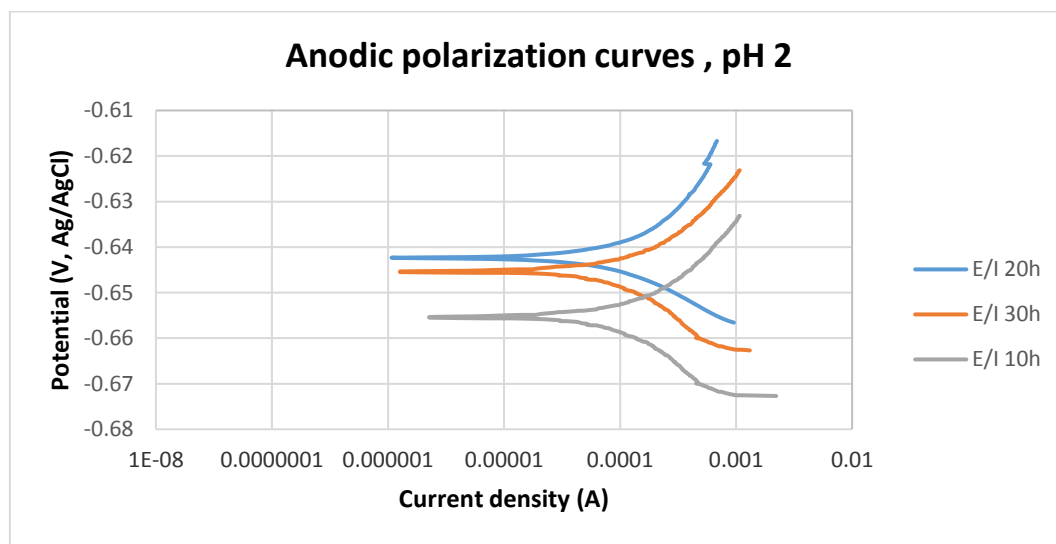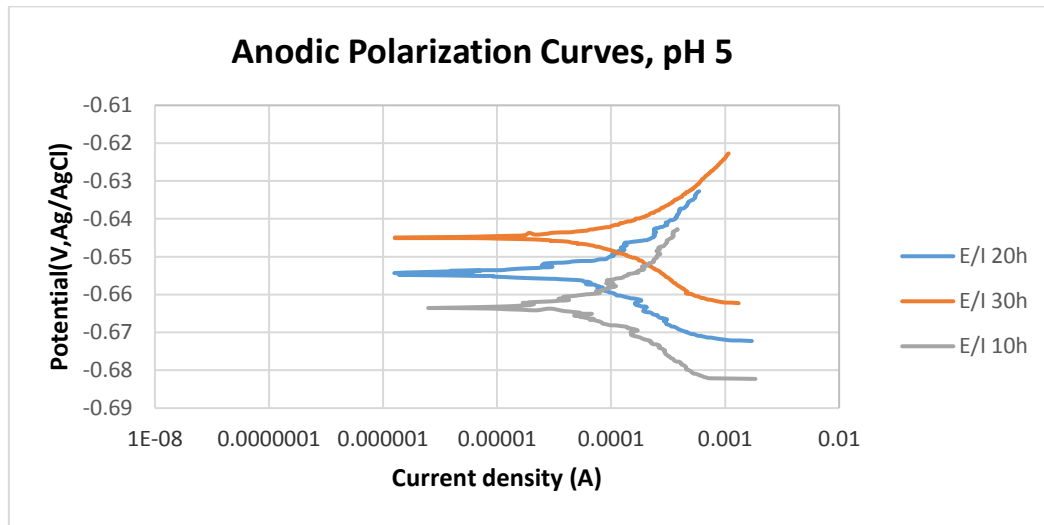


Figure 3. The potentiodynamic curves of 4130 Cr-Mo alloy steel covered with elemental sulfur in 3.5% sodium chloride solution at different immersion time: 10, 20 and 30 hours at pH 2.

Figure 3.also shows that $E_{corr}$ at pH 2 for 10 hours immersion time is the most negative one. It can be observed that current density 10 hours immersion is higher than that 20 and 30 hours immersion.

Figure 4.shows the stable behavior of anodic curves of samples covered with elemental sulfur with increasing the immersion time from 10 to 30 hours at 80 °C and pH 5. The potentiodynamic polarization curves indicate that $E_{corr}$ of 30 hours immersion is more positive than that of 20 hours immersion in the 3.5% sodium chloride solution. It can be observed

that current density of 20 hours immersion is higher than that of 30 hours immersion. The values of anodic ($\beta_a$) and cathodic ($\beta_c$) Tafel slopes of the samples of each experiments were determined as illustrated in Table 5.



Figure 4. The potentiodynamic curves of 4130 Cr-Mo alloy steel covered with elemental sulfur in 3.5% sodium chloride solution at different immersion time: 10, 20 and 30 hours at pH 5.

Table 5. The values of anodic ($\beta_a$) and cathodic ($\beta_c$) Tafel slopes of second series.

| Experiment | $\beta_a$ (mV.decade $^{-1}$) | $\beta_C$ (mV.decade $^{-1}$) |
|---|---|---|
| 7 | 0.032 | 0.015 |
| 8 | 0.030 | 0.013 |
| 9 | 0.023 | 0.020 |
| 10 | 0.022 | 0.021 |
| 11 | 0.022 | 0.019 |
| 12 | 0.020 | 0.019 |

**3.2.2 Corrosion rate of Cr-Mo low alloy steel**

The corrosion rates of second series of the experiments were calculated with the same method as first series. Table 6 indicates the corrosion rate of each experiments.

Table 6, the corrosion rate of second series.

| Experiment | 7 | 8 | 9 | 10 | 11 | 12 |
|---|---|---|---|---|---|---|
| pH | 2 | 2 | 2 | 5 | 5 | 5 |
| Corrosion Rate- CR (mm/year) | 0.615 | 0.605 | 0.595 | 0.381 | 0.367 | 0.318 |

As table 6 indicated, generally the corrosion rates of Cr-Mo alloy in presence of elemental sulfur are greater than those in presence of sulfide ions. Also, it can be observed that at pH 2 the rates of corrosion are higher than those of pH 5 which should be due to the formation of protective corrosion films on the alloy surface. The corrosion rate after 10 hours

immersion at pH 2 has its maximum of 0.615 mm/y which slightly decreased to 0.595 mm/y after 30 hours immersion. The corrosion rates of pH 5 gradually decreased by increasing immersion time due to the formation of protective corrosion layer. These results are consistent with data obtained from potentiodynamic polarization technique.

### 3.3 Analysis of corrosion products on the surface of the alloy

Figure.5 shows the SEM micrograph of the corrosion product films that form on the surface of each sample at pH 2 under 10, 20 and 30 hours immersion time in thioacetamide solution. From Figure.5 it can be said that by increasing immersion time, a thin corrosion layer gradually covered the alloy surface and protected it from further corrosion. EDS results indicate that this corrosion film contains iron sulfide and likely compounds of iron sulfide.
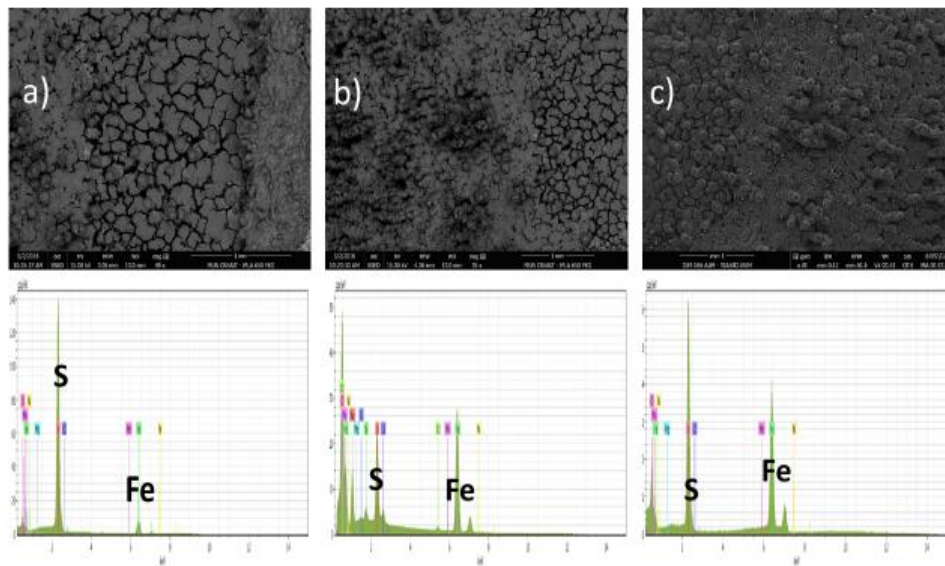


Figure 5. SEM micrograph and EDS of the corrosion product films that form on the surface of each samples at pH 2 under 10, 20 and 30 hours immersion time in thioacetamide solution.

Figure.6 shows the SEM micrograph of the corrosion product films that form on the surface of each sample at pH 5 under 10, 20 and 30 hours immersion time in thioacetamide solution.
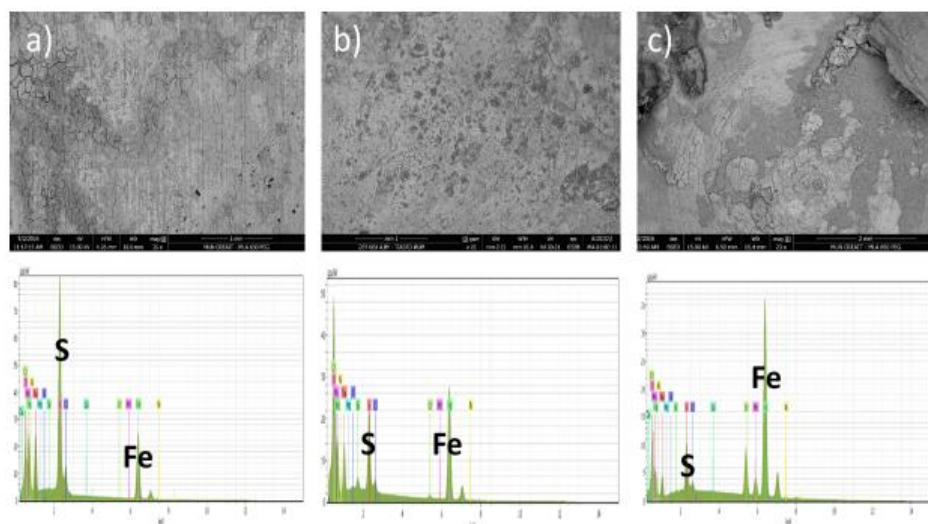
Figure 6. SEM micrograph and EDS of the corrosion product films that form on the surface of each samples at pH 5 under 10, 20 and 30 hours immersion time in thioacetamide solution.

Figure.6 (a) and (b) shows that generally, a much thicker film deposited on the alloy surface at pH 5 after 10 and 20 hours immersion in thioacetamide solution. The composition of this film was shown by EDS that consists of iron and sulfur. After 30 hours immersion in the solution, the corrosion layer was broken and exposed more unproductive alloy into the corrosive solution.

Figure.7 shows the SEM micrograph of the corrosion product films that form on the surface of each sample covered with elemental sulfur at pH 2 under 10, 20 and 30 hours immersion time.
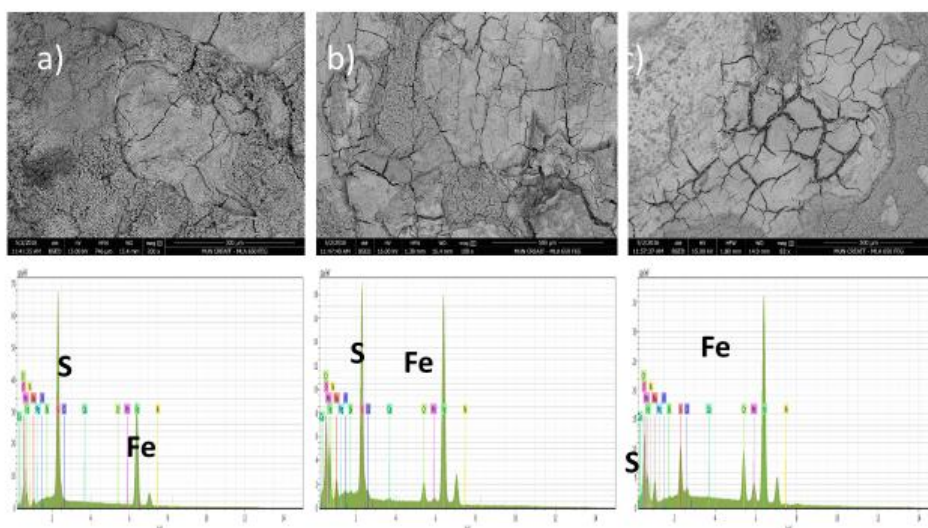


Figure 7. SEM micrograph and EDS of the corrosion product films that form on the surface of each samples covered with elemental sulfur at pH 2 under 10, 20 and 30 hours immersion time.

Figure. 7 illustrated that the highest percentage of cracks and pits can be observed in this experimental conditions, however, the corrosion products formation on the alloy surface gradually increased with the passage of time which slightly reduced the corrosion rate. The EDS analysis shows the presence of different values of iron and sulfur which will indicate the presence of various compounds of iron sulfide on the surface of samples as well.

Figure. 8 shows the SEM micrograph of the corrosion product films that form on the surface of each sample covered with elemental sulfur at pH 5 under 10, 20 and 30 hours immersion time.
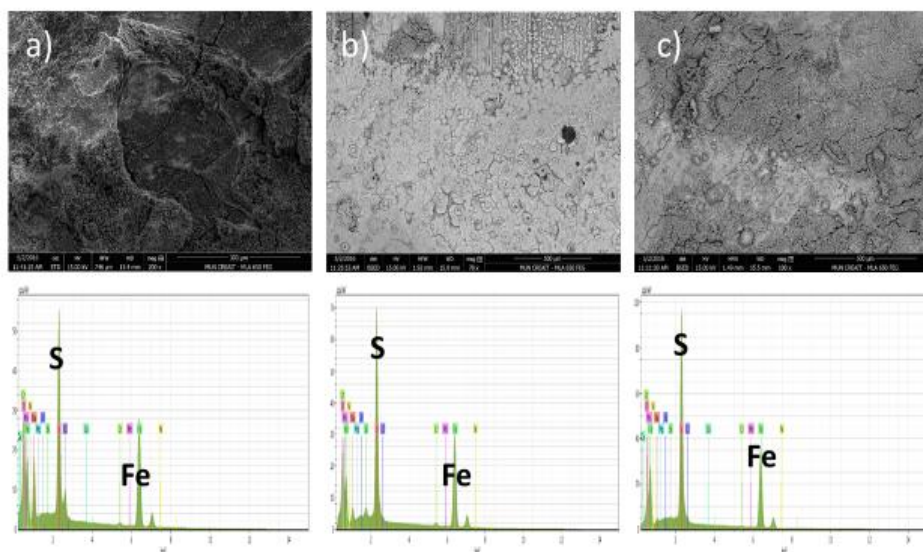


Figure 8. SEM micrograph of the corrosion product films that form on the surface of each samples covered with elemental sulfur at pH 5 under 10, 20 and 30 hours immersion time.

Comparison of Figure. 7 and 8 show that by increasing pH from 2 to 5 the corrosion film became more even and continuous which is consistent with data from corrosion rate and potentiodynamic polarization tests. At pH 5 and after 30 hours immersion in the solution, the corrosion films became finer and compact, indicative of good protection to the alloy compare to that of 10 and 20 hours immersion. Formation of this condensed corrosion film slightly prevents from further corrosion and consequently decreases the corrosion rate with the passage of time.

4. **Conclusion:**

- Corrosion resistance of Cr-Mo alloy in presence of elemental sulfur is significantly lower than its resistance in presence of sulfide ions with the same experimental conditions.
- Increasing the pH significantly decreases the corrosion rate of Cr-Mo alloy steel in the presence of elemental sulfur which is due to the formation of more even and compact corrosion films on the alloy surface.
- Effect of immersion time on the corrosion behavior of alloy is more complicated than the effect of pH. Results suggest that a number of factors such as microstructure, composition, and stability of corrosion products, immersion time can increase or decrease the corrosion rate.
- How stable are the corrosion products from elemental sulfur corrosion in various aggressive environments needs to be further investigated.

**References:**

[1]     H. Fang, D. Young, and N. Srdjan, "Elemental solfur corrosion of mild steel at high concentration of sodium chloride," *Int. Corros. Congr.*, vol. 2592, pp. 1–16, 2009.

[2]     J. Bojes, J. Lerbscher, W. Wamburi, C. Dilley, W. A. Blvd, and C. Dilley, "E;lemntal sulfur in 3-phase sour gas systems- is condensate really your alloty?," *NACE Int.*, pp. 1–22, 2010.

[3]     R. Steudel, "Mechanism for the Formation of Elemental Sulfur from Aqueous Sulfide in Chemical and Microbiological Desulfurization Processes," *Ind. Eng. Chem. Res.*, 1996.

[4]     P. . Boden and S. . Maldonado-Zagal, "Hydrolysis of Elemental Sulfur in Water and its Effects on the

Corrosion of Mild Steel," *Br. Corros. J.*, vol. 17, pp. 116–120, 1982.

[5]     D. . MacDonald, B. Roberts, and J. . Hyne, "The Corrosion of Carbon Steel by Wet Elemental Sulfur," *Corros. Sci.*, 1978.

[6]     H. Fang, B. Brown, D. Young, and S. Nesic, "Investigation of elemntal sulfur corrosion mechanisms," *NACE Int.*, no. 11398, pp. 1–13, 2011.

[7]     *NACE MR0175 / ISO 15156-1 Petroleum and natural gas industries — Materials for use in H 2 S-containing Environments in oil and gas production*, vol. 2001. .

[8]     H. Fang, "Investigation of Localized Corrosion of Carbon Steel in H2S Environments," *PhD Thesis, Ohio Univ.*, 2012.

[9]     W. Sun, "KINETICS OF IRON CARBONATE AND IRON SULFIDE SCALE FORMATION IN CO2/H2S CORROSION," *PhD Thesis, Ohio Univ.*, 2006.

[10]    D. G. Enos and L. L. Scribner, "The Potentiodynamic Polarization Scan Technical Report 33," *Cent. Electrochem. Sci. Eng.*, pp. 1–13, 1997.

[11]    ASTM-G5-82, "Standard reference method for making potentiostatic and potentiodynamic anodic polarisation measurements.," *Annu. B. ASTM Stand.*, vol. 03.02, no. Reapproved as ASTM-65–87 and as ASTM- 65–94, pp. 511–521, 1982.

[12]    W. Sun, N. Srdjan, and S. Papavinas, "KINETICS OF IRON SULFIDE AND MIXED IRON SULFIDE/CARBONATE SCALE PRECIPITATION IN CO2/H2S CORROSION," *NACE Int.*, vol. Paper No. , 2006.

[13]    K. J. Lee and S. Nesic, "A MECHANISTIC MODELING OF CO2 CORROSION OF MILD STEEL IN THE PRESENCE OF H2S," *PhD thesis*, no. 05630, pp. 1–16, 2004.

[14]    R. O. Rihan, "Electrochemical Corrosion Behavior of X52 and X60 Steels in Carbon Dioxide Containing Saltwater Solution," *Mater. Res.*, vol. 16, no. 1, pp. 227–236, 2013.

[15]    M. Koteeswaran, "CO 2 and H 2 S Corrosion in Oil Pipelines," *Master Thesis, Univ. Stavanger*, no. June, 2010.